

Investigating flexural and impact resilience of hybrid epoxy nanocomposites reinforced with carbon black – silica nanofiller

Joshua, R. M.

Department of Mechanical Engineering, Modibbo Adama University, Yola, Adamawa state, Nigeria

Paper History

Received: 10th June, 2024

Accepted: 11st July, 2024

Published: July, 2023

Abstract:

The mechanical performance of epoxy nanocomposites is crucial for their application in advanced engineering fields, yet enhancing their strength, stiffness, and impact resistance remains a challenge. This research investigates the flexural and impact resilience of hybrid carbon black-silica nanofiller-reinforced epoxy nanocomposites. This study seeks to determine the optimal composition and processing conditions that maximize mechanical performance by systematically varying the content and ratio of carbon black and silica nanoparticles. The production process involved preheating epoxy resin, incorporating nanofillers, and thorough mixing, followed by curing and characterization through flexural and impact tests adhering to ASTM standards. Response surface methodology was utilized to optimize the experimental design. The results indicated that combining thermally and chemically treated carbon black with silica nanoparticles significantly enhanced the mechanical properties. Specifically, the optimal nanocomposite exhibited a flexural strength increase from 65 MPa (pure epoxy) to 105 MPa and an impact resistance improvement from 0.5 kJ/m² (pure epoxy) to 1.3 kJ/m². Microstructural analysis via SEM confirmed a homogeneous nanofillers dispersion, contributing to the observed improvements. It is recommended to further explore these nanocomposite formulations for their potential in diverse engineering applications, ensuring high performance and resilience.

Corresponding author

Joshua, R. M.

raphbari@googlemail.com

Keywords: Carbon black, Flexural, Hybrid, Impact, Nanocomposite, Nanofiller, Silica

1. Introduction

The recent development in advanced materials with superior mechanical properties has become increasingly crucial in materials science and engineering. [1]. Nanocomposites have developed into an auspicious solution across various engineering applications in the quest for advanced materials with superior mechanical properties [2-4]. During the past few decades, thermosets have gained widespread utilization as essential structural and engineering materials [4-6]. Epoxy resins (ER) are thermoset polymers and are known for their excellent adhesion, chemical resistance, and thermal stability [7, 8], they form the matrix in which nanofillers are embedded to improve overall performance. Epoxy nanocomposites, known for their remarkable strength, stiffness, and thermal stability, have garnered significant attention for a wide range of industrial applications, including aerospace [9], automotive, and construction industries. Enhancing the mechanical performance of these nanocomposites by incorporating nanofillers has emerged as a promising strategy to meet the growing demands for high-performance materials [10]. One factor that causes fracture in engineering materials is considered to be low resistance to impact, flexural or fatigue strength [11] and how to reinforce brittle polymers [10] without affecting other important properties is a long-standing challenge [12]. Many researchers have carried out the flexural fatigue behavior of

composites and nanocomposites [13] and have studied the impact properties of epoxy-based nanocomposite

Nanofillers or Nanoparticles are the most basic components in the production of nanostructures, with sizes in the nanometer (1 nm = 10⁻⁹ m) range [1]. Nanoparticles remain a generally accepted reinforcement to most polymer matrices owing to their potential to reinforce polymers. Their high aspect ratio and large surface area improve the mechanical and thermal properties of polymer nanocomposites [4, 14] in comparison to conventional composites [15] at considerably low loading fractions owing to their greater interaction with the matrix [1]. Among the various nanofillers, carbon black (CB) and silica nanoparticles have demonstrated exceptional potential in reinforcing epoxy matrices [16]. Carbon black, with its high aspect ratio and excellent electrical conductivity [17, 18], offers substantial enhancements in mechanical strength and toughness to the host matrix [19, 20]. On the other hand, silica nanoparticles, known for their high surface area and strong interfacial bonding with the epoxy matrix, contribute to enhanced stiffness and thermal stability. The synergistic effect of combining these nanofillers can potentially lead to hybrid nanocomposites with superior mechanical properties [1, 21, 22]. However, Loading these nanoparticles is vital, and determining the suitable concentration is challenging [23, 24].

This study aims to investigate the flexural and impact resilience of hybrid carbon black silica nanofiller-reinforced epoxy nanocomposites. By systematically varying the content and ratio of carbon black and silica nanoparticles, this research seeks to elucidate the optimal composition and processing conditions that maximize the mechanical performance of the nanocomposites. Advanced characterization techniques, including flexural testing and impact resistance measurements, will be employed to assess the mechanical behavior and resilience of the hybrid nanocomposites. The findings from this study are expected to provide valuable insights into the design and optimization of epoxy nanocomposites for advanced engineering applications. By understanding the interplay between nanofiller content, distribution, and interfacial interactions, this research will contribute to the progression of high-performance materials with tailored mechanical properties. Ultimately, the results of this investigation will pave the way for the practical implementation of hybrid carbon black silica nanofiller-reinforced epoxy nanocomposites in various industries, driving innovation and enhancing the performance of next-generation materials.

2. Methodology

2.1 Materials

The epoxy resin used was supplied by Smooth-On with the commercial name of EpoxAmite 100 Resin and 102 medium hardener. The 102 medium hardener consists of triethylenetetramine (TETA) with propylene oxide (50-55 %), polyoxopropylene triamine (POPTA) (20-25 %) and TETA (15-20 %). The CB nanoparticle was obtained from CABOT under the commercial name of VULCAN® XC72 with a volume resistivity of 6 Ω -cm at 23 °C. VULCAN® XC72 has an iodine number of 253 mg/g density of 1.7-1.9 g/cm³ and OAN of 174 cc/100g, The SiO₂ nanoparticle with 10-25 nm diameter was obtained from Zhengzhou Dongshen Petro Chemical Technology Co, Ltd. The analytical grade chemicals used for surface treatments of the nanoparticles include tetrasodium pyrophosphate (TSPP), formic acid (FA), 3 Isocyanatopropyltriethoxysilane (IPTES), 3-Aminopropyltrimethoxysilane (APTES) and isophorone diisocyanate (IPDI).

2.2 Production of ER-CB nanocomposite

Three variations of CB which include has received CB, thermally treated CB and chemically modified thermally treated CB are used as one of hybrid nanofillers. 170g of epoxy was poured into beaker and preheated for 30 minutes at 40 °C to improve viscosity. 20 % nano silica with respect to CB %wt was measured and added to the beaker containing 170g of epoxy. 10 ml of IPDI was measured using a syringe and placed into the epoxy containing beaker, also added is 1.5 ml of IPTES. The mixture was stirred manually until a homogenous mixture was achieved. 12.5 %wt of CB with respect to epoxy resin content was placed into another beaker containing 250 ml of acetone, 4.6 % of APTES with respect to %wt of CB was also added. 5 %wt of TSPP with respect to CB %wt was added to the acetone containing beaker, FA was added gradually using a syringe until the PH value of the mixture is 4. The content of the beaker is

manually mixed before the sonication process. Sonication was done with an ultrasonic cleaner model 008 with an ultrasonic power of 50 w and a frequency of 40 KHz. The sonication process proceeded for 15 minutes at a time and a break period of 2 minutes between intervals. After 60 minutes of sonication, the content of the beaker containing acetone was mixed with the content of epoxy-containing beaker in a new beaker, the content is stirred manually until a homogenous mixture was achieved.

The beaker was then placed on a magnetic stirrer, the temperature was set to 60 °C and the speed was adjusted to 950 rpm. The magnetic stirring was made for 60 minutes while maintaining the temperature at 60 °C to ensure proper dispersion. Further stirring was done by the use a mechanical mixer at 600 rpm for 30 minutes; the mechanical mixer use was a pensonic PM-112 hand mixer with an electrical power of 120 w and a 5-speed selection. After the mixing process, acetone was evaporated using a hot air blower and by increasing the temperature of the magnetic stirrer to 75 °C to guarantee thorough evaporation of the solvent. The sample was then placed in the degassing chamber; the vacuum pump was operated for 30 minutes to remove air bubbles trapped within the sample. The resin-hardener ratio of 100:29 as advised by the manufacturer was adopted; 49.3g of hardener was added to the degassed sample and blended manually till a homogenous mixture was attained. The nanocomposite was then transferred into the molds. The samples were post cured for 60 minutes at 100°C in an oven to complete the curing action the mold was designed according to ASTM D638 for the tensile strength samples and ASTM D695 for the compressive strength sample.

2.3 Experimental design

Response surface methodology was adopted to optimize the production of the nanocomposite; the empirical model was obtained using Box Behnken experimental design. One (1) categorical and four (4) numeric experimental factors (state of CB nanoparticle, magnetic stir Speed, magnetic stir time, CB weight fraction and silica weight fraction) were used in the research as shown in Table 1. Each response was measured according to the standards specified in Table 2. A total of 87 runs in a single block were used with 5 central points for each categoric factor as is typical with Box-Behnken experimental design.

Some of objectives of this research are to determine which factors are most significant on the response variables, and to determine where to set the dominant controllable factor so that the response is almost near the desired optimal value. The Design-Expert 10 software was used in the generation of the experimental design and the analysis of the interactions of the factors.

3 Result and Discussion

3.1 RSM and Data Analysis

Response surface methodology (RSM) is a collection of mathematical and statistical techniques for empirical model building by careful design of experiments, in order to optimize a response which is influenced by several input factors [25]. Design-Expert version 10 software was used to

create the design of experiment for the RSM and was also used to analyze the collected data. An output response was obtained in accordance to the experimental matrix of Table 1, the response data was keyed into the software for each

response. The software followed the inbuilt process as predefined by the program to determine the model equation and analyze the model to ensure its validity using statistical techniques.

Table 1: Experimental Factors and their Levels

Levels of Variables	Input Variables				
	Magnetic Stir Speed (rpm)	Magnetic Stir Time (Hours)	CB Weight Fraction (%wt)	Silica Weight Fraction (%wt)	State of CB Nanoparticle
1	700	1	5	0	As Received [1 0]
0	950	2.5	12.5	10	Thermally Treated [0 1]
+1	1200	4	20	20	Thermally & Chemically treated [-1 -1]

Table 2: Response Variables

S/No.	Response	Unit	Standard
1	Flexural Strength	MPa	ASTM D790
2	Impact Strength	KJ/m ²	ASTM D275

3.2 Flexural Strength Response Data

The Box-Cox transformation report from the software as shown in Figure 1 recommended an inverse square root transformation. The transformation is used to modify the distributional shape of the set of data to be more normally distributed so that tests and confidence limits that require normality can be appropriately used. The current lambda position is at 1 as shown in Figure 1 which is outside the low

confidence interval of -1.29 and the high confidence interval 0.5. The inverse square root transformation is use to place the lamda at -0.5 which is close to best lambda of -0.49 The Predicted Residual Sum of Squares (PRESS) for the Quadratic model is 2.437E-003; it is a measure of how well the quadratic model fits each point in the design. It has a higher R-square of 0.95 (as shown in Figure 1) except for the cubic model which is aliased; the predicted R-square of 0.92 is in logical agreement with the adjusted R-square since their difference is less than 0.2. The model equations for the flexural strength are as shown in equation (1) – (3).

$$1/\text{Sqrt}(Y_{flex(CB)}) = +0.18 - 4.80E-003 * A - 9.40E-005 * B - 2.05E-003 * C - 3.38E-003 * D - 5.70E-007 * AB + 1.85E-004 * AC + 1.16E-004 * AD + 6.05E-008 * BC + 2.79E-006 * BD - 2.78E-005 * CD - 6.80E-005 * A^2 + 3.81E-008 * B^2 + 2.17E-004 * C^2 + 2.75E-005 * D^2 \quad (1)$$

$$1/\text{Sqrt}(Y_{flex(CB600)}) = +0.18 - 4.62E-003 * A - 9.52E-005 * B - 2.27E-003 * C - 3.39E-003 * D - 5.70E-007 * AB + 1.85E-004 * AC + 1.16E-004 * AD + 6.05E-008 * BC + 2.79E-006 * BD - 2.78E-005 * CD - 6.80E-005 * A^2 + 3.81E-008 * B^2 + 2.17E-004 * C^2 + 2.75E-005 * D^2 \quad (2)$$

$$1/\text{Sqrt}(Y_{flex(CB-M)}) = +0.18 - 4.49E-003 * A - 9.52E-005 * B - 2.55E-003 * C - 3.38E-003 * D - 5.70E-007 * AB + 1.85E-004 * AC + 1.16E-004 * AD + 6.05E-008 * BC + 2.79E-006 * BD - 2.78E-005 * CD - 6.80E-005 * A^2 + 3.81E-008 * B^2 + 2.17E-004 * C^2 + 2.75E-005 * D^2 \quad (3)$$

Where: $Y_{flex(CB)}$ is the Flexural Strength of Epoxy-CB nanocomposite sample, $Y_{flex(CB600)}$ is the Flexural Strength of Epoxy-CB600 nanocomposite sample, $Y_{flex(CB-M)}$ is the Flexural Strength of Epoxy-CB-M nanocomposite sample while A, B, C and D are as previously defined

The equation can be used to predict the flexural strength of the nanocomposites for given level of each factor.

3.3 ANOVA for the Flexural Strength Data

The analysis of variance (ANOVA) for the flexural strength response data is shown in Table 4, ANOVA is vital in testing the significance and sufficiency of the model; it subdivides the total variation of the results in two sources of variation (model and experimental error). ANOVA shows whether the variation from the model is significant when compared to the variation due to residual error [26].

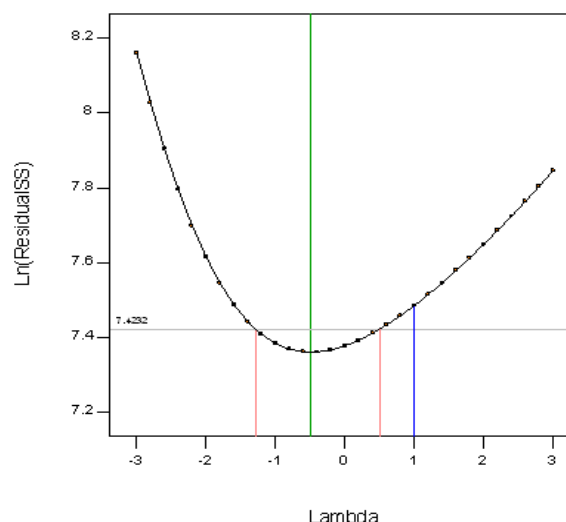


Figure 1: Box-Cox Plot for Power Transformation of the Flexural Strength Model

Table 3: Summary Statistics of Flexural Strength Model

Source	Standard Deviation	R-Squared	Adjusted R-Squared	Predicted R-Squared	PRESS	
Linear	7.872E-003	0.8003	0.7853	0.7637	5.865E-003	
2FI	7.972E-003	0.8310	0.7798	0.7017	7.403E-003	
Quadratic	4.330E-003	0.9532	0.9350	0.9018	2.437E-003	Suggested
Cubic	2.938E-003	0.9878	0.9692	0.9177	2.042E-003	Aliased

Table 4: ANOVA for the Regression Model of Equation 1 - 3

Source	Sum of Squares	Df	Mean Square	F-Value	p-value Prob > F
Model	0.024	24	9.858E-003	52.59	< 0.0001
A-Magnetic Stir Time	1.379E-003	1	1.379E-003	73.56	<0.0001
B-Magnetic Stir speed	5.343E-003	1	5.343E-003	2.85	0.0964
C-CB content	0.018	1	0.018	941.53	< 0.0001
D-Si Content	2.934E-004	1	2.934E-004	10.38	<0.0020
E-Modification	5.868E-004	2	2.934E-004	15.65	<0.0001
AB	5.490E-007	1	5.490E-007	0.029	0.8647
AC	5.188E-007	1	5.188E-007	0.028192	0.8684
AD	3.653E-005	1	3.653E-005	1.95	0.1677
AE	1.318E-006	2	6.589E-007	0.035	0.9655
BC	1.543E-007	1	1.543E-007	8.234E-003	0.9280
BD	5.858E-004	1	5.858E-004	31.25	<0.0001
BE	7.658E-007	2	7.658E-007	0.020	0.9798
CD	5.231E-005	1	5.231E-005	2.79	0.0999
CE	8.452E-005	2	2.226E-005	2.25	0.1135
DE	9.376E-008	2	4.688E-008	2.501E-003	0.9975
A ²	4.549E-007	1	4.549E-007	0.024	0.8767
B ²	1.103E-004	1	1.103E-004	5.88	0.0182
C ²	2.893E-003	1	2.893E-003	154.34	<0.0001
D ²	1.467E-004	1	1.467E-004	7.83	0.0068
Residual	1.162E-003	62	1.875E-005		
Lack of Fit	1.031E-003	50	2.063E-003	1.89	0.1144
Pure Error	1.031E-003	12	1.091E-005		
Cor Total	0.025	86			

F-value of the model is the ratio between the mean square of the model and the residual error [27], the F-value for the quadratic model is 52.59 as shown in Table 4. There is only a 0.01% chance that an F-value this large could occur due to noise. The significance of each term was determined by p-value (Prob> F), which is listed in Table 4, the terms A, C, D, E, BD, B², C² and D², were significant, with very small p-values ($p < 0.05$). "Adeq Precision" value is 27.560, it measures the signal to noise ratio. A ratio greater than 4 is desirable hence this model can be used to navigate the design space. The lack of fit F-value of 1.89 implies the lack of fit is not significant relative to the pure error. When the lack of fit is significant it suggests that there are factors, other than those considered by the model, that are affecting the response [26]. There is an 11.44% chance that a lack of fit F-value this large could occur due to noise. The response surface plots for the flexural strength are shown in Figures 3, 4 and 6, it is a trace plots revealing how the response changes when changing the proportion of each parameter while keeping some of the parameters constant.

The overall centroid has been used as points for the constant parameters in order to gain insights into the nanocomposite system. Figure 4 shows the response surface plot for the flexural strength of the nanocomposite at a constant magnetic stir speed of 950 rpm and SiO₂ loading of 10 %wt. Figure 2 shows the predicted verses measured flexural strength

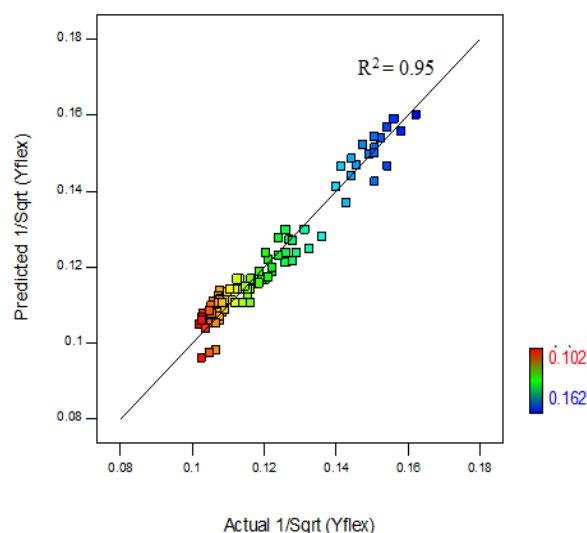


Figure 2: Plot of Predicted vs. Measured Flexural Strength

In the 3D plot, the interaction between the CB content and the magnetic stir time explains the behavior of the flexural strength of the nanocomposite. From a maximum flexural strength of 108 MPa at 5 %wt of CB-M using magnetic stir time of 4 hours, the flexural strength decreases with increasing CB-M %wt.

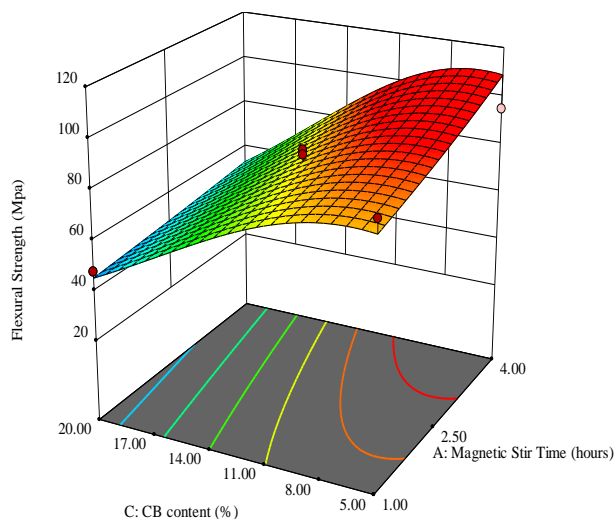


Figure 3: Response Surface Plots for the Flexural Strength of Epoxy/CB-M Nanocomposite at Magnetic Stir Speed of 950 rpm and 10 %wt. of SiO₂

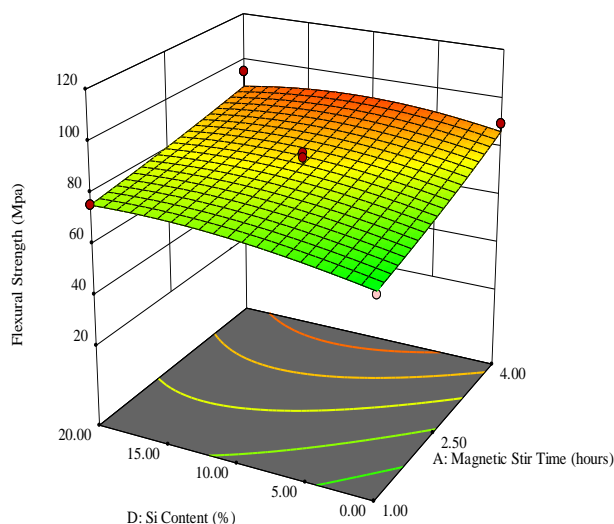


Figure 4: Response Surface Plots for the Flexural Strength of Epoxy/CB-M Nanocomposite at Magnetic Stir Speed of 950 rpm and 12.50 %wt of CB-M

This could be attributed to the dispersion of nanoparticles which is optimal in the 5 %wt. CB-M content,

because the morphology images and dispersion of nano-fillers were better as shown in Figure 5, which led to stronger interfacial adhesion between matrix and fillers. the increase in magnetic stir time improves the flexural strength of the epoxy/CB-M nanocomposite at all levels of the CB content. Figure 4 shows the response surface plot of the flexural strength of the nanocomposites at a magnetic stir speed of 950 rpm and a CB-M loading of 12.50 %wt. The figure shows the effect of varying the SiO₂ content and the magnetic stir time on the flexural strength of the nanocomposites. The interaction explains the increase of flexural strength of the epoxy/CB-M nanocomposite with increase in the magnetic stir time in the absence of SiO₂. The synergistic effect of adding the SiO₂ while increasing the magnetic stir time has the effect of increasing the flexural strength to a maximum of 95 MPa.

Figure 6 shows the response surface plot of the flexural strength of epoxy/CB-M nanocomposite at magnetic stir speed of 950 rpm and magnetic time of 2.50 hours while varying the SiO₂ content and the CB %wt. As previously observed increasing the CB content reduces the flexural strength of the epoxy/CB-M nanocomposites from a 44 MPa at 20 %wt in the absence SiO₂. Adding SiO₂ has the effect of increasing the flexural strength of the nanocomposite at all level of the CB content, the synergistic effect of the SiO₂ and CB content improves the flexural strength of the nanocomposite to a maximum of 92 MPa.

Figure 7 shows the effect of the interaction between the Magnetic stir speed and the SiO₂ content on the flexural strength of the nanocomposite, at a magnetic stir time of 2.50 hours and 12.5 %wt. of CB-M. The interaction between the magnetic stir speed and the SiO₂ content is very significant because of a high F-value of 31.25 and a low p-value of <0.0001 as shown in Table 4. At 1200 rpm (magnetic stir speed) the flexural strength decreases with increase in SiO₂ content this anomaly was also confirmed by Pullicino, *et al.* [28]. The expectation is that higher speeds such as 1200 rpm will form smaller average agglomerates than the 700 rpm, hence better nanofiller/matrix interaction with consequent improved mechanical properties, which is not the case. However at 700 rpm, the flexural strength of the nanocomposite improves with increase in the SiO₂ content.

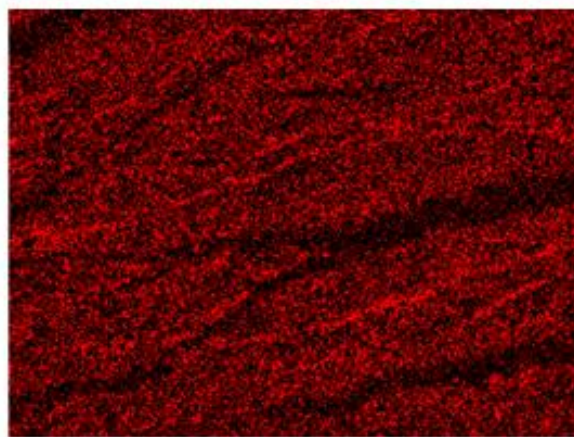
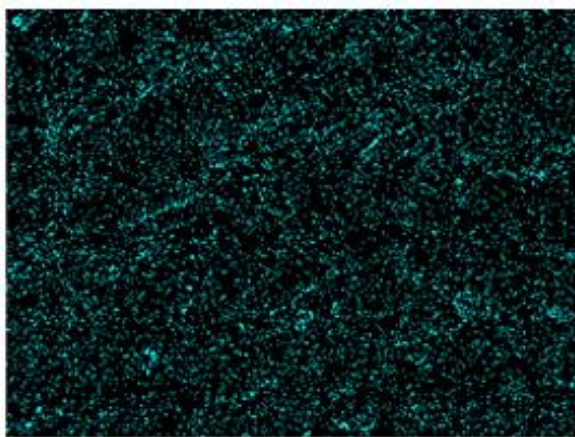


Figure 5: (a) SiO₂ Nanoparticle and (b) CB-M Nanoparticle Mapping in Epoxy Resin-Carbon Black-Silica Nanocomposite

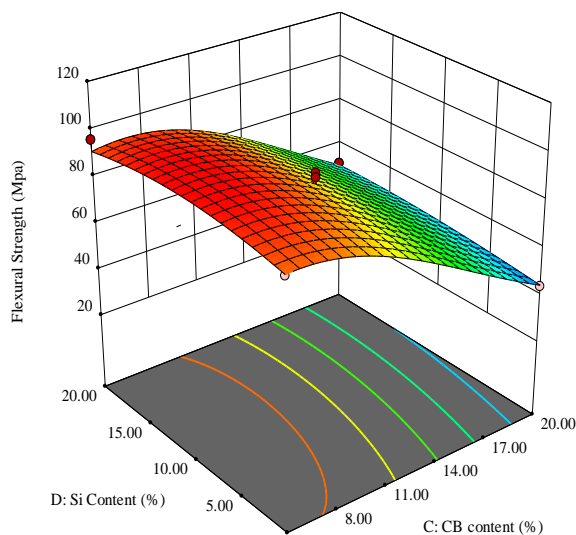


Figure 6: Response Surface Plots for the Flexural Strength of Epoxy/CB-M Nanocomposite at Magnetic Stir Speed of 950 rpm and Magnetic Stir Time of 2.50 hours

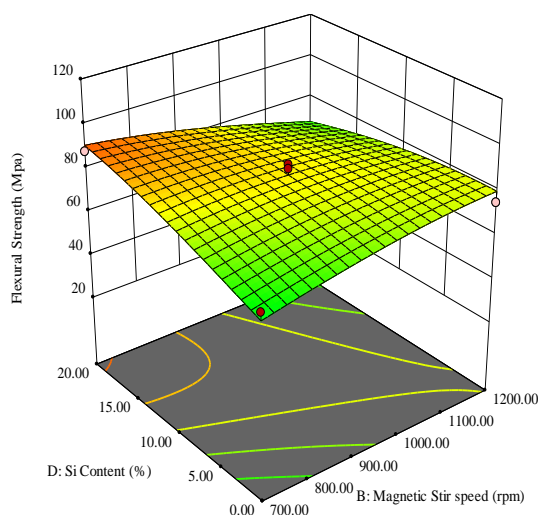


Figure 7: Response Surface Plots for the Flexural Strength of Epoxy/CB-M Nanocomposite at Magnetic Stir Time of 2.50 hours and 12.50 %wt. of CB-M

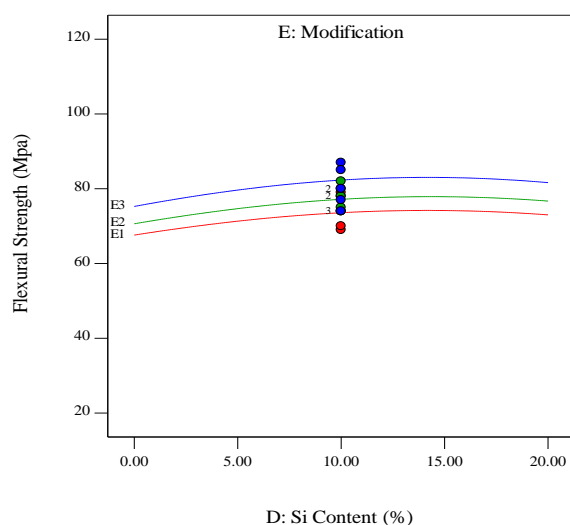


Figure 8: Interaction Effect Plot of SiO₂ Content and Modification of CB nanoparticle on Flexural Strength

Figure 8 shows the effect of the interaction between the silica content and the CB nanoparticle modification on the flexural strength of the nanocomposite. Similar trend as was observed in the compressive strength of the nanocomposite is seen for the flexural strength of the nanocomposite. Thermal modification of the CB nanoparticle has better and improved effect on the flexural strength of the nanocomposite than as received CB nanoparticle.

Figure 9 also shows the effect of modification of the nanoparticle on the flexural strength as the CB content increases, similar trend of better flexural strength with modification is observed with subsequent decrease in the flexural strength of the nanocomposite as the CB content increases.

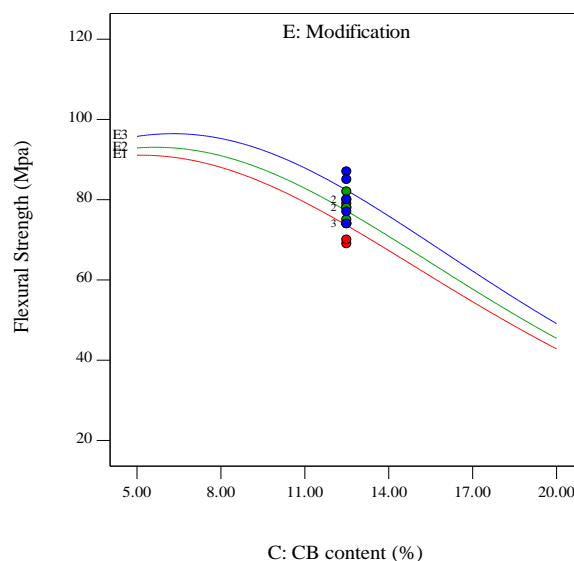


Figure 9: Interaction Effect Plot of CB Content and Modification of CB Nanoparticle on Flexural Strength

The result of characterization of the nanoparticle as shown in Figure 10 indicate an improvement with the presence of functional group on the surface of CB nanoparticle. This modification of the nanocomposite containing the modified CB nanoparticle has improved flexural strength at all levels of the parameters.

Figure 11 shows a significant interaction between the magnetic stir speed and the SiO₂ content as shown in ANOVA Table of 4. The interaction has an F-value of 31.25 and a low p-value of <0.0001, the figure shows a much-improved flexural strength at 700 rpm with the addition of SiO₂. This effect reduces as the magnetic stir speed increases from 700 – 1200 rpm, a better flexural strength of 94 MPa was observed at 700 rpm with the addition of SiO₂.

4. Statistical Analysis of the Impact Strength Response Data

From Table 5 PRESS for the quadratic model is 244.72; the model has an R-square of 0.96, the predicted R-square is 0.8053 and is in logical agreement with the adjusted R-square since their difference is less than 0.2. The polynomial model equations for the flexural strength are:

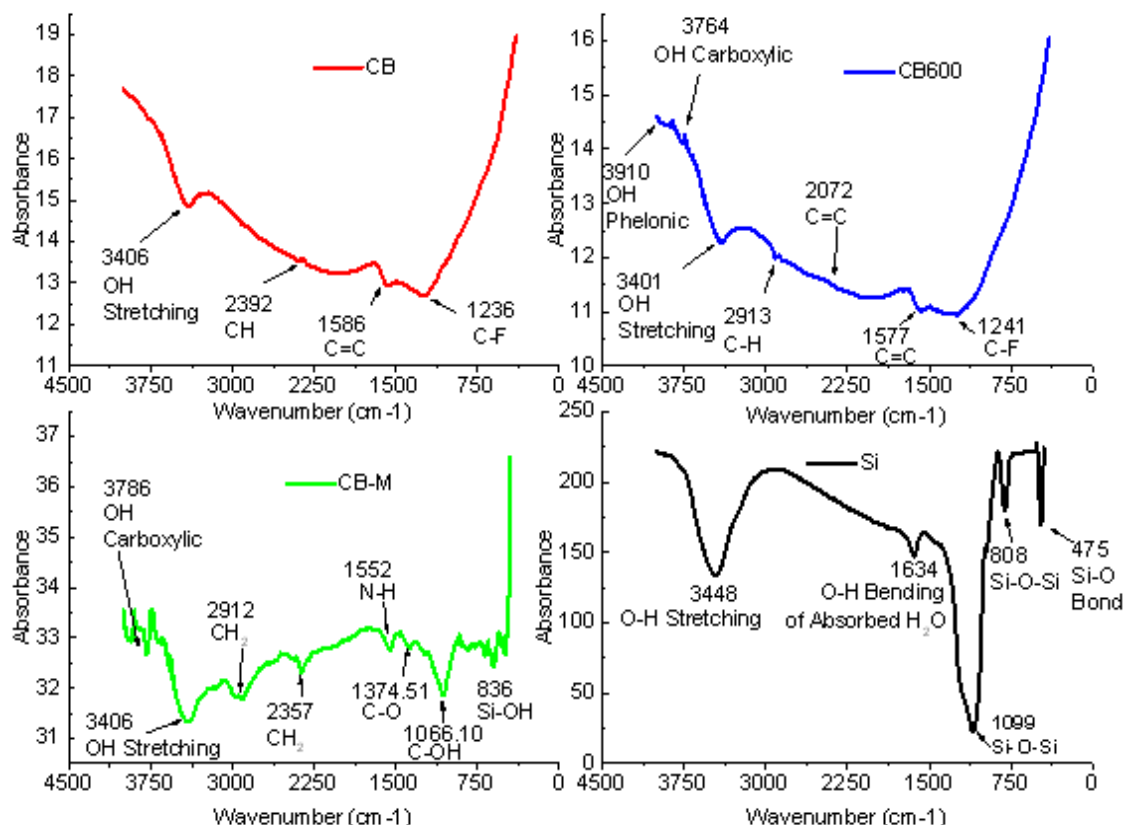


Figure 10: FTIR of the Nanoparticles (a) as Received CB (b) Thermally Treated CB at 600 °C (c) Thermally Treated CB at 600 °C followed by Chemical Modification (d) Silica

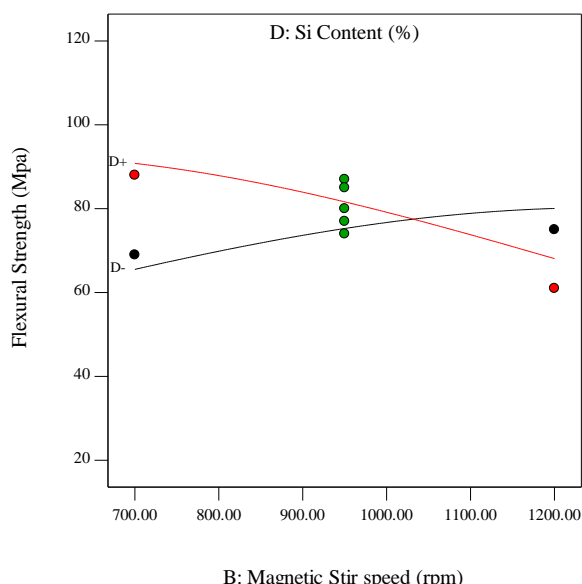


Figure 11: Interaction Effect Plot of Magnetic Stir Speed and SiO₂ Content on Flexural Strength

Impact Strength of Epoxy-CB-M Nanocomposite sample A, B, C and D are as previously defined. Results obtained after carrying out ANOVA is presented in Table 6, values of "Prob. > F" less than 0.05 indicate the model terms are significant. Values greater than 0.10 indicate the model terms are not significant. A model F-value of 59.89 and a very low p-value (Prob > F) of < 0.0001 indicate a significant model fit. From the regression model of impact strength of the nanocomposite, the model terms B, C, D, E, A², B² and C² were significant with a probability of 95%. The "Lack of Fit" F-value of 0.78 implies that there is insignificant lack of fit. The "Lack of Fit" (Prob > F) value of 0.74 implies that there is only 74 % chance that the "Lack of Fit" F-value could occur due to noise.

Figure 12 shows the measured values versus the predicted values of impact strength of the nanocomposite using the second order polynomial of equations 4 – 6. The regression model equations provided a very precise explanation of the experimental data, showing that it was successful in capturing the correlation between the process parameters that describe the impact strength.

Table 5: Summary Statistics of Impact Strength Model

Source	Standard Deviation	R-Squared	Adjusted R-Squared	Predicted R-Squared	PRESS	
Linear	2.51	0.8374	0.8252	0.8053	601.17	Suggested Aliased
2FI	2.71	0.8429	0.7953	0.7040	914.08	
Quadratic	1.44	0.9587	0.9426	0.9208	244.72	
Cubic	1.36	0.9797	0.9487	0.8716	396.46	

$$Y_{imp}(CB) = +24.27 - 4.06 * A - 0.02 * B + 0.55 * C + 0.47 * D - 8.89E - 004 * AB - 1.57 * AC - 0.01 * AD + 2.67E - 004 * BC - 1.33E - 004 * BD - 7.78E - 003 * CD + 0.97 * A^2 + 1.09E - 005 * B^2 - 0.06 * C^2 + 5.56E - 004 * D^2 \quad (4)$$

$$Y_{imp}(CB600) = +28.64 - 4.16 * A - 0.02 * B + 0.55 * C + 0.47 * D - 8.89E - 004 * AB - 1.57 * AC - 0.01 * AD + 2.67E - 004 * BC - 1.33E - 004 * BD - 7.78E - 003 * CD + 0.97 * A^2 + 1.09E - 005 * B^2 - 0.06 * C^2 + 5.56E - 004 * D^2 \quad (5)$$

$$Y_{imp}(CB-M) = +31.47 - 4.11 * A - 0.02 * B + 0.62 * C + 0.43 * D - 8.89E - 004 * AB - 1.57 * AC - 0.01 * AD + 2.67E - 004 * BC - 1.33E - 004 * BD - 7.78E - 003 * CD + 0.97 * A^2 + 1.09E - 005 * B^2 - 0.06 * C^2 + 5.56E - 004 * D^2 \quad (6)$$

Where: $Y_{imp}(CB)$ is the Impact Strength of Epoxy-CB Nanocomposite sample, $Y_{imp}(CB600)$ is the Impact Strength of Epoxy-CB600 Nanocomposite sample, $Y_{imp}(CB-M)$ is the

Strength of Epoxy-CB-M Nanocomposite sample A, B, C and D are as defined in Table 4

Table 6: ANOVA Table for the Regression Model of Equation 4 - 6

Source	Sum of Squares	Df	Mean Square	F-Value	p-value Prob > F
Model	2960.73	24	123.36	59.86	< 0.0001
A-Magnetic. Stir Time	4.00	1	4.00	1.94	0.1684
B-Magnetic Stir speed	28.44	1	28.44	13.61	0.0004
C-CB content	812.25	1	812.25	394.34	< 0.0001
D-Si Content	164.69	1	164.69	79.96	< 0.0001
E-Modification	1576.99	2	788.49	382.81	< 0.0001
AB	1.33	1	1.33	0.65	0.4241
AC	0.000	1	0.000	0.000	1.0000
AD	0.33	1	0.33	0.16	0.6889
AE	0.17	2	0.083	0.040	0.9604
BC	3.00	1	3.00	1.46	0.2321
BD	1.33	1	1.33	0.65	0.4241
BE	3.72	2	1.86	0.90	0.4104
CD	4.08	1	4.08	1.98	0.1641
CE	2.00	2	1.00	0.49	0.6177
DE	0.89	2	0.44	0.22	0.8065
A ²	92.53	1	92.53	44.92	< 0.0001
B ²	9.01	1	9.01	4.38	0.0406
C ²	188.35	1	188.35	91.44	< 0.0001
D ²	0.060	1	0.060	0.029	0.8650
Residual	127.71	62	2.06		
Lack of Fit	97.71	50	1.95	0.78	0.7400
Pure Error	30.00	12	2.50		
Cor Total	3088.44	86			

The R-square of 0.96 showed that the unpredictability in the impact strength of 96 % could be explained by the second order polynomials and only 4 % of the total impact strength variations were not explained by the independent variables of the polynomials.

Figure 13 shows the impact strength response behavior of the epoxy nanocomposites system in relation to the interaction between the Magnetic stir speed and CB-M %wt. loading. The observed trend is the progressive decrease in the values of the impact strength with increasing %wt. of CB-M. This behavior can be attributed to better dispersion of the nanofiller at lower viscosity of the liquid epoxy before hardening

Figure 14 shows the response of the impact strength of the nanocomposite to the interaction between SiO₂ and magnetic stir speed. The *t*-test shows that this interaction contribute slightly to the increase in the impact strength of the nanocomposite as shown by the p-value of 0.4241 in Table 6.

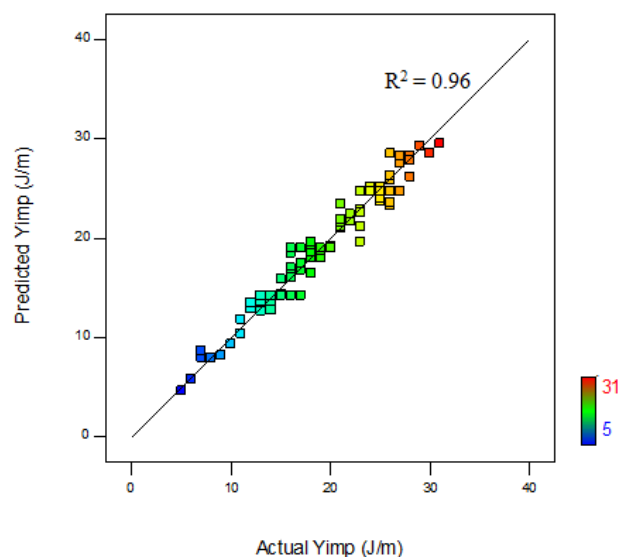


Figure 12: Plot of Predicted vs. Measured Impact Strength

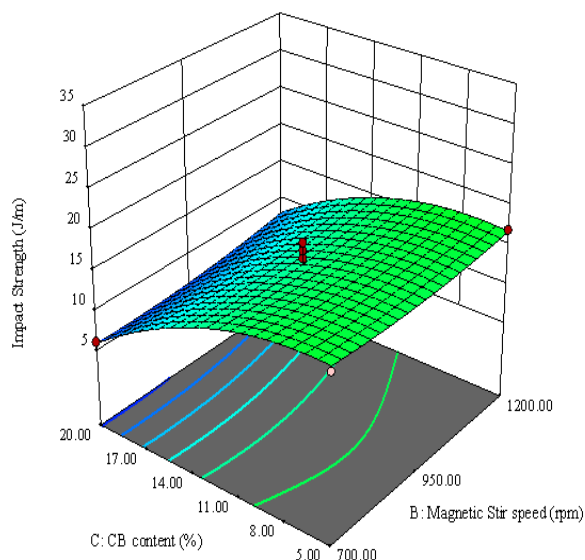


Figure 13: Response Surface Plots for the Impact Strength of Epoxy/CB-M Nanocomposite at Magnetic Stir Time of 2.50 hours and 10 %wt. of SiO₂

The effect of increase in the magnetic stir speed on the impact strength is much noticeable at higher SiO₂ %wt. loading.

Figure 15 shows favoring of the load transfer between the CB-M and the resin, which leads to a high-impact energy absorption. The impact strength increases with the reduction of the %wt. of CB-M, and it is attributed to increase in agglomeration with increase in the %wt. CB-M. Interaction effect of CB-M content and modification of CB on the impact strength of the nanocomposite. An increase in the impact strength of the nanocomposite is observed as the treatment of nanoparticle progress from thermal treatment to thermal-chemical treatment. The high values for the impact strength may be related to the functionalization of CB-M nanoparticles, which in this case can be attributed to the covalent bonds between the amine groups present in the CB-M-hardener.

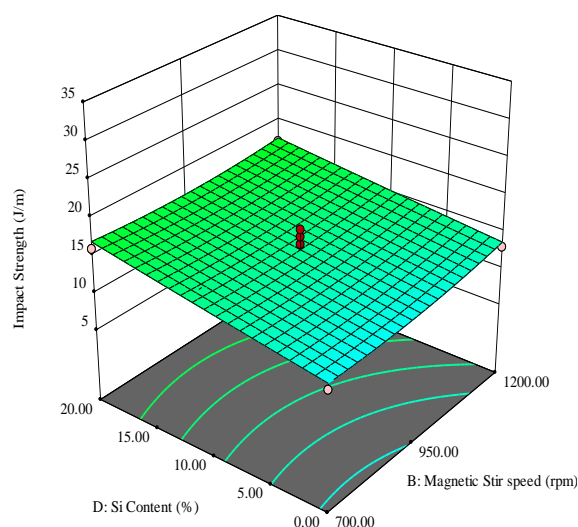


Figure 14: Response Surface Plots for the Impact Strength of Epoxy/CB-M Nanocomposite at Magnetic Stir Time of 2.50 hours and 12.5 %wt. of CB-M

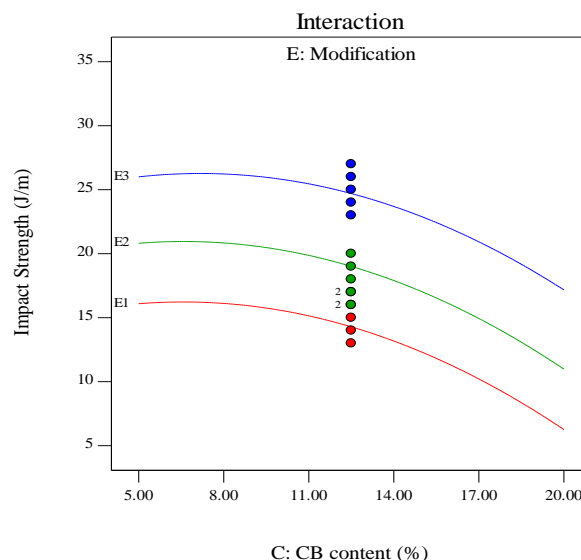


Figure 15: Interaction Effect Plot of CB-M Content and Modification of CB Nanoparticle on Impact Strength

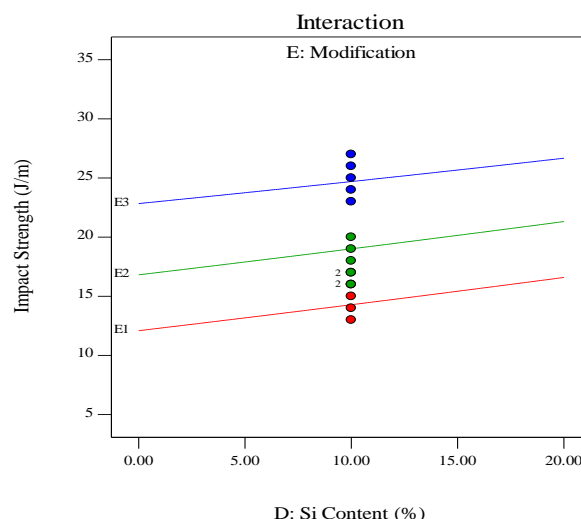


Figure 16: Interaction Effect Plot of SiO₂ Content and Modification of CB Nanoparticle on Impact Strength

Also the epoxy groups present in the resin [29], the hardener molecules covalently linked to an epoxy system increase the mobility of the polymer chains.

Figure 16 shows the response of the impact strength of the nanocomposite to the interaction between the modification of the CB nanoparticle and the %wt. of SiO₂. The impact strength of the nanocomposite is observed to increase with increase the addition of SiO₂. The synergistic effect of the modification of the CB nanoparticle and the addition of SiO₂ is improved impact strength of the nanocomposite.

5. Conclusion

This study successfully evaluated the mechanical performance of hybrid carbon black-silica nanofiller-reinforced epoxy nanocomposites, demonstrating significant enhancements in both flexural strength and impact resistance. Through a methodical approach that involved varying the content and ratios of carbon black and silica nanoparticles, and using response surface

methodology for optimization, the research identified the optimal nanocomposite formulation. The best-performing nanocomposite achieved a notable flexural strength increase from 65 MPa for pure epoxy to 105 MPa and an impact resistance enhancement from 0.5 kJ/m² to 1.3 kJ/m². The microstructural analysis confirmed a uniform dispersion of nanofillers, which is critical to these improvements. These findings suggest that the integration of thermally and chemically treated carbon black with silica nanoparticles effectively boosts the mechanical properties of epoxy nanocomposites. This opens new avenues for their application in areas demanding high mechanical performance and resilience. Future work should focus on exploring the long-term durability and environmental stability of these nanocomposites, as well as scaling up the production process for industrial applications. This research provides a strong foundation for further development and application of advanced nanocomposite materials in engineering and technology sectors.

References

- [1]. Anand, A. and Joshi, M., (2015). Structural Composites Hybridized with Nanofillers: An Overview. *Journal of the Indian Institute of Science*, 95(3), 1- 17.
- [2]. Alam, M. N., Kumar, V., Jeong, T. and Park, S. S., (2023). Nanocarbon Black and Molybdenum Disulfide Hybrid Filler System for the Enhancement of Fracture Toughness and Electromechanical Sensing Properties in the Silicone Rubber-Based Energy Harvester. *Polymer*, 15(2189), 1 - 14.
- [3]. Amjad, A., Rahman, A. A. A., Awais, H., Abidin, M. S. Z. and Khan, J., (2022). A Review Investigating the Influence of Nanofiller Addition on The Mechanical, Thermal and Water Absorption Properties of Cellulosic Fibre, *Journal of Industrial Textile*, 51(1S), 65S–100S.
- [4]. Jung, J., (2022). Functionalized Aramid Nanofibers for the Reinforcement of Thermosets and Rubber Nanocomposites, PhD Thesis in *Macromolecular Science and Engineering*, University of Michigan.
- [5]. Dong, M., Tomes, O., Soul, A., Hu, Y., Bilotti, E., Zhang, H. and Papageorgiou, D. G., (2024). Hybrid Ti3C2Tx MXene and Carbon Nanotube Reinforced Epoxy Nanocomposites for Self-Sensing and Structural Health Monitoring. *ACS Applied Nano Materials*, 7, 3314–3325.
- [6]. Medupin, R. O., Abubakre, O. K., Abdulkareem, A. S., Muriana, R. A. and Abdulrahman, A. S., (2019). Carbon Nanotube Reinforced Natural Rubber Nanocomposite for Anthropomorphic Prosthetic Foot Purpose, *Scientific Reports, Nature Research*, 9(20146), 1-11.
- [7]. Namdev A., Telang A. and Purohit R., (2022). Experimental Investigation on Mechanical and Wear Properties off GNP/Carbon Fiber/Epoxy Hybrid Composites, *Materials Research Express*, 9(025303), 1 - 16.
- [8]. Bajpai, A., Martin, R., Ibarboure, E. and Faria, H., (2020). Epoxy Based Hybrid Nanocomposites: Fracture Mechanisms, Tensile Properties And Electrical Properties, *Materials Today: Proceedings*, 34(1), 210-216.
- [9]. Wazalwar, R., Sahu, M. and Raichur, A. M., (2021). Mechanical Properties Of Aerospace Epoxy Composites Reinforced with 2d Nano-Fillers: Current Status And Road to Industrialization, *Royal Society of Chemistry, Nano Scale Advances*, 3(2741), 1 - 36.
- [10]. Jin, F. L. and Park, S. J., (2008). Impact-Strength Improvement of Epoxy Resins Reinforced with a Biodegradable Polymer. *Materials Science and Engineering (A)*, 478, 402–405.
- [11]. Kanie, T., Fujii, K., Arikawa, H. and Inoue, K., (2000). Flexural Properties and Impact Strength of Denture Base Polymer Reinforced With Woven Glass Fibers, *Dental Materials*, 16, 150–158.
- [12]. Ye, Y., Chen, H., Wu, J. and Ye, L., (2007). *High Impact Strength Epoxy Nanocomposites with Natural Nanotubes*. Elsevier Polymer, 48, 6426 - 6433.
- [13]. Shokrieh, M. M., Esmkhani, M., Haghighatkah, A. R. and Zhao, Z., (2014). Flexural Fatigue Behavior of Synthesized Graphene/Carbon-Nanofiber/ Epoxy Hybrid Nanocomposites, *Materials and Design*, 62, 401–408.
- [14]. Hashim, U. R., Jumahat, A. and Jawaid, M., (2021). Mechanical Properties of Hybrid Graphene Nanoplatelet-Nanosilica Filled Unidirectional Basalt Fibre Composites, *Nano Materials*, 11(1468), 1 - 17.
- [15]. McBride, A. K., Turek, S. L., Zaghi, A. E. and Burke, K. A. (2017). Mechanical Behavior of Hybrid Glass/Steel Fiber Reinforced Epoxy Composites, *Polymer*, 9(151), 1 - 16.
- [16]. Bajuria, F., Mazlana, N., Ishaka, M. R. and Imatomib. J., (2015). *Flexural and Compressive Properties of Hybrid Kenaf/Silica Nanoparticles in Epoxy Composite*. In 5th International Conference on Recent Advances in Materials, Minerals and Environment (RAMM) & 2nd International Postgraduate Conference on Materials, Mineral and Polymer (MAMIP), held 4th -6th August Selangor, Malaysia, pp. 1-12
- [17]. Kumar, V., Alam, M. N., Manikkavel, A., Song, M., Lee, D. J. and Park, S. S., (2021). Silicone Rubber Composites Reinforced by Carbon Nanofillers and Their Hybrids for Various Applications: A Review. *Polymer*, 13(2322), 1 - 31.
- [18]. Majeed, A. H., Hamza, M. S. and Kareem, H. R., (2014). Effect of Adding Nanocarbon Black on the Mechanical Properties of Epoxy. *Diyala Journal of Engineering Sciences*, 07(01), 94-108.
- [19]. Bera, T., Acharya, S. K. and Mishra, P., (2018). Synthesis, mechanical and thermal properties of carbon black/epoxy composites, *International Journal of Engineering, Science and Technology*, 10(4), 12 - 20.
- [20]. Knoll, J. B., Riecken, B. T., Kosmann, N., Chandrasekaran, S., Schulte, K. and Fiedler, B., (2014). *The Effect of Carbon Nanoparticles on The Fatigue Performance of Carbon Fibre Reinforced*

- Epoxy. *Composites*, Part A, 67(2014), 233–240.
- [21]. Megahed, M., Megahed, A. A. and Agwa, M. A., (2018). Mechanical Properties of On/Off-Axis Loading for Hybrid Glass Fiber Reinforced Epoxy Filled With Silica and Carbon Black Nanoparticles, *Materials Technology Advanced Performance Materials*, 2018,1-9.
- [22]. Megahed, M., Megahed, A. A. and Agwa, M. A., (2019). The Influence of Incorporation of Silica and Carbon Nanoparticles on the Mechanical Properties of Hybrid Glass Fiber Reinforced Epoxy. *Journal of Industrail Textile*, 49(2), 181 - 199.
- [23]. Zena, Y. G., Woldemariam, M. H. and Koricho, E. G., (2023). Nano-Additives and Their Effects on the Microwave Absorptions and Mechanical Properties of the Composite Materials, *Manufacturing Review*, 10(8), 1 - 16.
- [24]. Woldemariam, M. H., Belingardi, G., Koricho, E. G. and Reda, D. T., (2019). Effects Of Nanomaterials And Particles On Mechanical Properties and Fracture Toughness of Composite Materials: A Short Review. *AIMS Materials Science*, 6(6), 1191–1212.
- [25]. Myers, R. H., Montgomery, D. C. and Anderson-Cook, C. M. (2016). *Response Surface Methodology*:. Fourth ed. Wiley Series in Probability and Statistics, New York, United States of America: Wiley. 821.
- [26]. Segurola, J., Allen, N. S. Edge, M. and Mahonb, A. M. (1999). Design of Eutectic Photoinitiator Blends for Uv/Visible Curable Acrylated Printing Inks and Coatings, *Progress in Organic Coatings*, 37, 23-37.
- [27]. Kasiri, M. B., Modirshahla, N. and Mansouri, H. (2013). Decolorization of Organic Dye Solution by Ozonation; Optimization with Response Surface Methodology, *International Journal of Industrial Chemistry*, 4(3), 1-10.
- [28]. Pullicino, E., Zou, W., Gresil, M. and Soutis, C., (2017). The Effect of Shear Mixing Speed and Time on the Mechanical Properties of GNP/Epoxy Composites, *Applied Composite Materials*, 24(2017), 301–311.
- [29]. Gao, J., Li, J. Benicewicz, B. C. Zhao, S. Hillborg, H. and Schadler, L. S., (2012). The Mechanical Properties of Epoxy Composites Filled with Rubbery Copolymer Grafted SiO₂. *Polymers*, 4, 187-210.